FERMILAB-PUB-25-0497-LBNF-STUDENT

Identification of the Liquid Argon Scattering Experimental Discrepancies Using Simulation

Auto Breaux[a)]

(*Electronic mail: abreaux8@tulane.edu.)

(Dated: 7 August 2025)

Scintillation light analysis in liquid argon based neutrino detectors is restrained in capability due to uncertainty in fundamental constants critical to the analysis process. One such property is the Rayleigh scattering length of liquid argon. In the fall of 2023, the TallBo cryostat, located in the Noble Liquid Testing Facility (NLTF) at Fermilab, was used to study the scattering length of liquid argon in the Liquid Argon Scattering (LArS) experiment. Due to systematic errors unknown during measurement analysis, LArS's measurements were quite uncertain. By simulating the LArS experiment, we found that the downturn in detector count rate as a function of liquid argon height at low heights was caused by a misplaced silicon photo multiplier (SiPM). With concentrated effort, we may be able to successfully correct this effect by understanding the relationship between the specified Rayleigh scattering length and the measured attenuation length. With this information and further progression in analysis, we may be able to extract corrected measurements from the LArS data and attain a tangible experimental measurement of the scattering length of liquid argon.

I. INTRODUCTION

We aim to simulate the LArS experiment to understand the unexpected trend reversal seen in the experimental data and to know how to correct for this during data analysis. By accounting for any discrepancies, we can make the first direct measurement of the total attenuation length in liquid argon as a function of wavelength. This measurement will improve the simulation and reconstruction of scintillation light in large liquid argon experiments like DUNE.

II. BACKGROUND

The Deep Underground Neutrino Experiment (DUNE)[1] will be a massive liquid argon based neutrino detector located approximately one mile beneath the Sanford Underground Research Facility. DUNE's primary physics goals include determining the neutrino mass hierarchy and measuring the CP violating phase, but its capabilities will span far beyond these two objectives. In order to have the ability to span multiple areas of study within neutrino physics, DUNE must be able to detect any trace an interacting neutrino leaves, including photon emissions. DUNE will use Silicon Photo Multipliers (SiPM) to detect such emissions. Optimizing our understanding of the photon detectors in DUNE reduces uncertainty in the experiment's measurements, and allows the photon detection mechanism to realize its full potential. In order to constrain uncertainties associated with the photon detectors, we must also understand photon behavior within liquid argon. One presently poorly measured value that is critical to detector optimization is the Rayleigh scattering length of liquid argon. Constraining this value will push DUNE toward achieving its science goals.

The LArS experiment[2] was performed using the TallBo cryostat located in the NLTF at Fermilab. During experimentation, the interior of this cylindrical cryostat contained a cage that was lined with 10 SiPMs – 8 along the side and 2 on the bottom. Most relevant to our simulations, the bottom SiPMs were intended to lie 8.75 cm to the right of the center to align with the light source. Fig. 1 depicts a schematic of the LArS experiment. Before any given data acquisition period, TallBo was filled with liquid argon. After the volume was filled with liquid argon to the maximum fill level, light with a selected monochromatic wavelength was emitted downward into the cryostat via a 5 mm x 5 mm source that lied 8.75 cm to the right of the center. Data was taken as the liquid argon level was lowered in a controllable manner, yielding results at specified liquid argon heights alongside the known, controlled wavelengths.

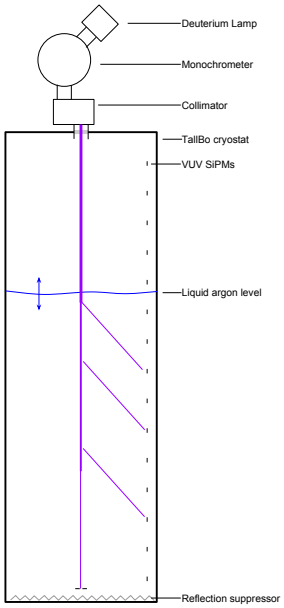

FIG. 1. LArS Experiment Schematic

[a)]Also at Physics Department, Tulane University.

This manuscript has been authored by FermiForward Discovery Group, LLC under Contract No. 89243024CSC000002 with the U.S. Department of Energy, Office of Science, Office of High Energy Physics.

The Beer-Lambert law states that the probability P of finding any given photon at depth x in liquid argon, where L is the attenuation length of liquid argon [described by Eq. (2)], is

$$P(x) \propto e^{-\frac{x}{L}} \tag{1}$$

The relationship between the attenuation length L, the Rayleigh scattering length L_s, and the absorption length L_a of liquid argon is

$$\frac{1}{L} = \frac{1}{L_s} + \frac{1}{L_a} \tag{2}$$

For measurements at different wavelengths and liquid argon depths, the Rayleigh scattering length ratio R at 90°, where I is the scattered intensity, I_0 is the incident intensity, r is distance from the scattering center to the detector, and V is the scattering volume, is

$$R = \frac{I}{I_0}\frac{r^2}{V} \propto \frac{1}{L_s^4} \tag{3}$$

The relationship between the SiPM trigger rate and the SiPM depth was mapped at a wavelength of 128 nm, as shown in Fig. 2. Eq. (1) and Eq. (2) predict a constantly decreasing exponential behavior with increasing depth in the measurement of the SiPM trigger rate as a function the SiPM depth. Unexpectedly, the trend of the SiPM trigger rate reverses between 0 cm to 40 cm.

The relationship between the SiPM trigger rate and the SiPM depth at a wavelength of 180 nm was measured too, as seen in Fig. 3. Unexpectedly, the count rate persistently increases throughout the domain of SiPM depths. This behavior is not predicted by Eq. (1) and Eq. (2).

With predictable behavior in the relationship between the SiPM trigger rate and the SiPM depth, we could perform a fit to the exponential curve and extract an attenuation length. With knowledge of the value of L_a, or accounting for it in analysis, we can extract the scattering length of a given wavelength of light in liquid argon using this relationship via Eq. (2).

By simulating the LArS experiment, performing analysis, and making comparisons with the measurements of the experiment, we can stride toward understanding the cause of these behaviors and accounting for them. This would yield an extractable measurement of the Rayleigh scattering length of liquid argon.

III. SETUP

Geant4[3][4][5] is a powerful toolkit that is used to simulate particles passing through matter. We used Geant4 v4.10.6.p01c to simulate the LArS experiment, as it is well equipped with the tools needed to mimic the most critical components of the experiment.

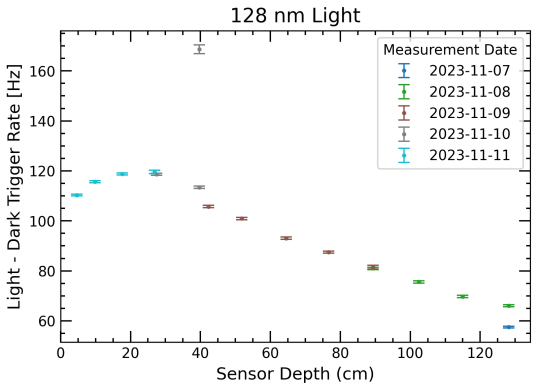

FIG. 2. SiPM Trigger Rate vs. SiPM Depth at 128 nm

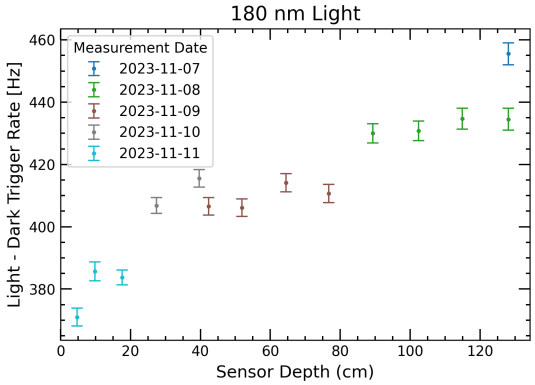

FIG. 3. SiPM Trigger Rate vs. SiPM Depth at 180 nm

First, we constructed the detector volume using GDML files. This provided us with the malleability to specify traits of the volumes associated with the LArS experiment. Critically, we could nearly identically recreate the TallBo cryostat, the removable cage, the SiPM detectors attached to the cage, the liquid argon filling the cryostat, and the gaseous argon into which the liquid argon evaporates. Notable volume traits specified include the size, shape, position, and matter composition, which were all meticulously selected to mimic the as-built reality of LArS depicted in Fig. 1.

Also relevant to our simulations, Geant4 allowed us to specify a multitude of material properties such as the refractive indices, scattering lengths, absorption lengths, and other optical properties of materials. We specified the index of refraction of liquid argon to be 1.358 at all wavelengths. We specified the absorption length of liquid argon to be 100 m at all wavelengths to nullify its potentially skewing effect on the simulated data. We specified the scattering length of liquid argon to be 90 cm at a wavelength of 128 nm based on the theoretical predictions of Seidel, Lanou, and Yao[6], then predicted the remainder of the wavelengths' associated scattering lengths based on Eq. (3).

Aside from implementing our detector geometry and making toolkit-required initializations, we inherited and customized necessary Geant4 classes to simulate the most important nuances of LArS. This includes the particle type, the particle source and its location, and initial particle properties such as wavelength and momentum direction. Simultaneously, we use these classes for data acquisition, as they have the capacity to emulate and output the data extracted in the physical experiment.

After acquiring the simulation data produced by Geant4, we require a powerful toolkit to handle our analysis work. We use ROOT[7] v6.20.08a for this, as it has the capacity to extract and present the results we desire efficiently.

The Geant4 simulation and ROOT analysis code used in this paper is publicly accessible in the LArSMC Github repository[8].

IV. METHODS

For access to a detailed view and understanding of the positional distribution of photons that traversed TallBo, we chose to store data on simulated photons that hit the bottom of the cage and the bottom SiPMs. This included the final coordinates of the photon and its distance from the center of the simulated bottom SiPMs. With this data, we had more information on the relationship between the photon position distributions and the liquid argon height.

V. RESULTS

Our simulations reveal that as the liquid argon height increases, the photons are distributed more evenly across the bottom of the cage. Due to this decrease in the concentration of photons directly underneath the light source, the bottom SiPMs – located directly underneath the light source in our simulations – detect fewer photons. Physically, this relationship can be attributed to Rayleigh scattering events in the liquid argon, as a scattering event is more likely to occur if a given photon has more matter to traverse prior to hitting the bottom of the cage.

The aforementioned relationship between the photon position distribution and the liquid argon height seen in our simulations suggests that the bottom SiPMs should have the highest count rate at the lowest liquid argon heights in the physical experiment. However, this is not what was observed as shown previously in Fig. 2. This contrast suggests that the bottom SiPMs were not properly aligned within the cryostat.

To predict the location of the bottom SiPMs, we can splice the bottom of the cage into rings and observe the behavior of the photon position distribution as a function of liquid argon height at different distances from a center coordinate. As seen in Fig. 4, we chose rings surrounding the center of the bottom projection of the photon source. The rings all have 3 mm of distance between their inner and outer radii. If the bottom SiPMs fall within one of these analysis rings in the physical experiment, the ring data and the LArS data would present very similar total photon count / photon count rate versus liquid argon height behavior at the respective ring since the radial distances would overlap.

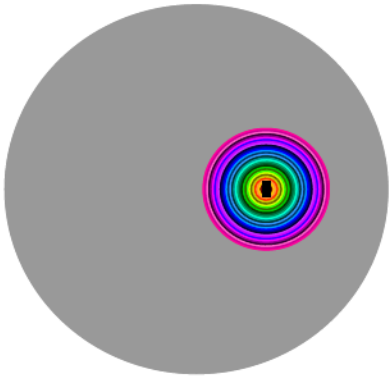

FIG. 4. Schematic of Radial Distance Intervals on TallBo Bottom. Each ring's respective color corresponds to the same color's curve and range in Fig. 5.

Our renderings of total photon count as a function of liquid argon height at radial intervals greater than 6 mm exhibited similar behavior to the 128 nm experimental data as seen in Fig. 5. This finding implies that the bottom SiPMs were misaligned in the experiment and were not directly under the light source as intended.

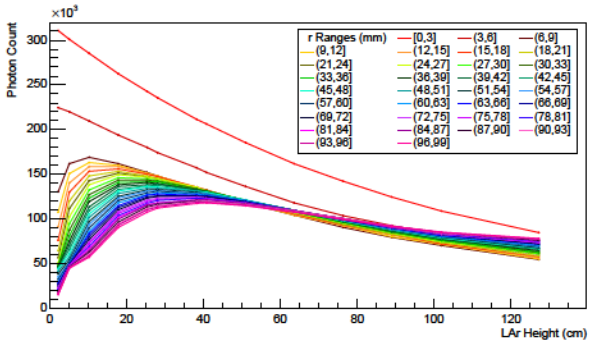

FIG. 5. Total Photon Count vs. Liquid Argon Height (cm) at 128 nm. The R = [0,3] range is decreased by a factor of 300. The R = (3,6] range is decreased by a factor of 6.

In an attempt to correct for the misplacement of the bottom SiPMs, we journeyed two distinct analysis routes: tail-end attenuation length extraction and correction and a broad likelihood ratio test.

A. Tail-End Analysis

Motivated by attaining a general, sweeping correction for the experimental data, we performed a tail-end analysis of our simulation data. In the tail-end analysis method, we extracted the tail end of the simulated photon count as a function of the liquid argon height (presented in Fig. 5) at different radial

distance and liquid argon height intervals, and then fit it to a variable exponential function. The exponential fitting analysis yields an extractable attenuation length by the Beer-Lambert law stated in Eq. (1). To retrieve the most consistent and precise attenuation lengths from these fits, we needed to meticulously select a constant liquid argon height range to fit over. More specifically, the fits' liquid argon height range needed to consistently measure nearest to the specified Rayleigh scattering length. This emulates the predicted relationship between the two seen in Eq. (2) best, as we specified the absorption length of liquid argon relatively high to nullify its effect. We sampled many liquid argon height ranges with varying minima and then investigated the minima's relationship with each fit's extracted attenuation length. The results are depicted in Fig. 6.

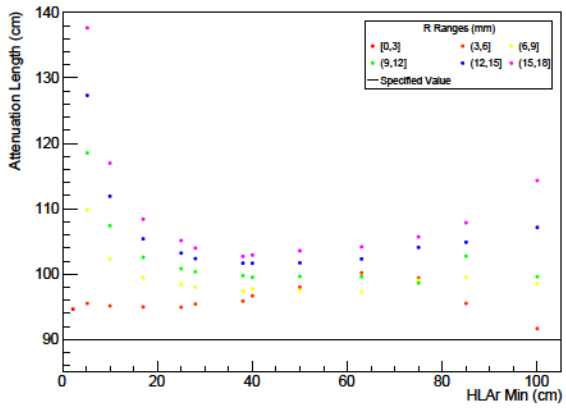

FIG. 6. Extracted Attenuation Length (cm) vs. Liquid Argon Height Minimum (cm) at a wavelength of 128 nm

After concluding that the most consistently promising liquid argon height range choice was 38 cm to 128 cm, we performed the same exponential fitting analysis at multiple scattering lengths and relevant radial distances in this liquid argon height range as shown in Fig. 7. Here, the maximum scattering length correlates to a wavelength of 155 nm as predicted by Eq. (3). These results may signify a defined relationship between the specified Rayleigh scattering length and the extracted attenuation length. If this relationship is uncovered with further analysis, we may be able to generalize data correction.

B. Likelihood Ratio Test

Motivated by attaining a best fit to the existing data for specifiable attenuation length extraction, we performed a likelihood ratio test. In this second method of analysis, we extracted the chi squared of the fits of all the possible combinations of specified wavelength and radial distance intervals' weighted total photon counts versus liquid argon height to the experimentally measured photon count rate versus SiPM depth at a wavelength of 128 nm (presented in Fig. 2). The results of this test are presented in Fig. 8, and the resulted best

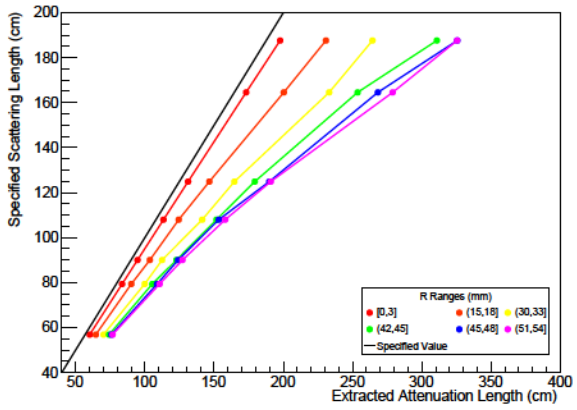

FIG. 7. Specified Rayleigh Scattering Length (cm) vs. Total Attenuation Length (cm) in the liquid argon height range of 38 cm to 128 cm. Note: Fig. 6 and Fig. 7 specify different r ranges.

fit plotted with the experimental data is presented in Fig. 9. With this information, we could perform an exponential fit to the best fit's total photon count versus the liquid argon height for photons detected by the simulated bottom SiPMs at their intended placements, then extract an attenuation length by the Beer-Lambert law stated in Eq. (1).

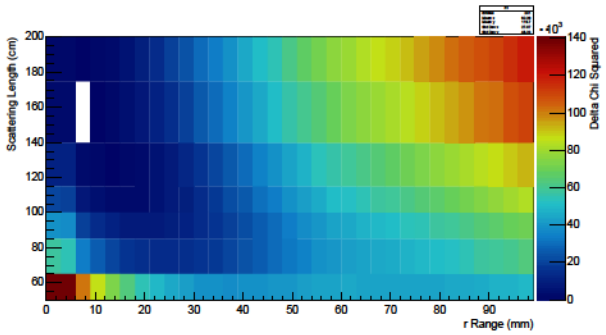

FIG. 8. Delta Chi Squared as a function of Scattering Length and Radial Distance. The chi squared values result from fits to the experimental data presented in Fig. 2.

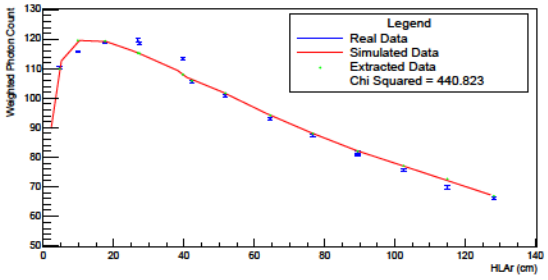

FIG. 9. Weighted Photon Count vs. Liquid Argon Height (cm) at a wavelength of 150 nm and radial distance interval of 6 mm to 9 mm plotted alongside the 128 nm experimental data.

Notice, though, that the best fit presented in Fig. 9 has a relatively drastic reversal in photon count compared to the experimental data. In an attempt to understand this behavior, we utilized a grid-based analysis method instead of a ring-based analysis method. With a grid of 1 mm by 1 mm squares and information on the amount of photon detections within those squares lining the bottom of the TallBo cage, we could reconstruct the SiPMs at any position. This was motivated by the suspicion that the position of the bottom SiPMs within each ring could affect the data due to the geometrical asymmetry prevalent in Fig. 4. We chose to reconstruct eight 6 mm by 6 mm SiPMs at a randomly selected distance from the center of the bottom projection of the photon source of 15 mm. Each of these was positioned at different azimuthal angles in intervals of $\frac{\pi}{4}$ from the x axis. The results of this analysis are presented in Fig. 10.

We suspect that the gap in total photon count at lower liquid argon heights that alternates between sequential azimuthal angles is due to the method we reconstructed the detector with. During analysis, we did not rotate the reconstruction of the SiPMs, so at $\frac{\pi}{4}$, $\frac{3\pi}{4}$, $\frac{5\pi}{4}$, and $\frac{7\pi}{4}$ radians, the nearest point to the center of the bottom projection of the photon source is a vertex of the reconstructed SiPM, while at 0, $\frac{\pi}{2}$, π, and $\frac{3\pi}{2}$ radians, the closest point to the center of the bottom projection of the photon source is one of the side's midpoint. This may slightly vary the total photon count, though direct analysis is required to prove this assumption.

Based on our grid analysis, it is evident that the radial positioning of the SiPMs is relatively insignificant at equal distances from the center of the source's projection. Furthermore, if we select the 0 and $\frac{\pi}{4}$ radian curves and plot them alongside the experimental data and the ring-based analysis data near 15 mm, it is evident that the grid-based analysis results do not clearly emulate the behavior of the experimental results more than the ring-based analysis results. This can be realized in Fig. 11.

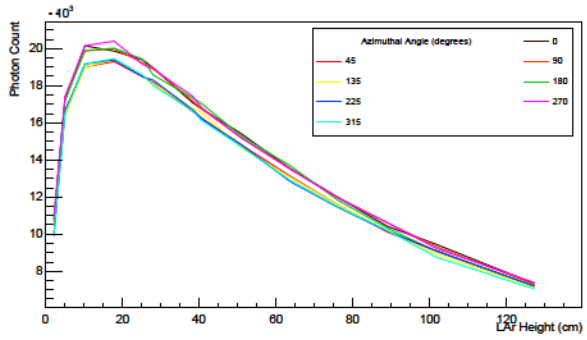

FIG. 10. Total Photon Count vs. Liquid Argon Height in reconstructed SiPMs at different azimuthal angles with a wavelength of 128 nm.

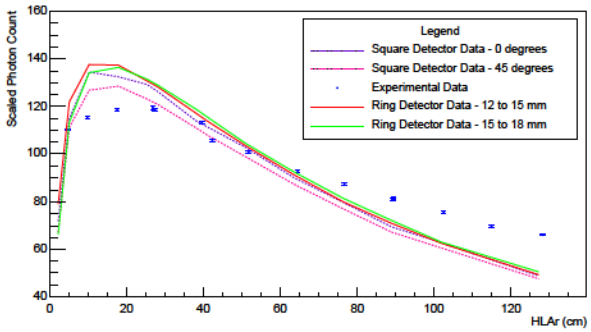

FIG. 11. Plot of the grid-based and ring-based weighted Total Photon Count vs. Liquid Argon Height relationships alongside the experimental data at a wavelength of 128 nm.

VI. CONCLUSION

Using simulation to interpret the LArS experimental results, we discovered the cause of the unexplained turnover at lower liquid argon heights: misaligned bottom SiPMs. In one analysis framework, we mapped the relationship between the extracted attenuation length and the specified scattering length in our simulations. In another method of analysis, we realized the best specifications for simulating LArS that grant us the ability to make a direct measurement of the total attenuation length in liquid argon as a function of scattering length. Finally, we discovered that there are no prevalent differences in the results of a Cartesian-based and radial-based analysis for our simulations.

VII. FUTURE OBJECTIVES

Our simulations could be immediately improved by specifying the absorption length of the liquid argon, the reflective properties of the cage, and the divergence of the particle source to Geant4.

Both analysis frameworks presented in this paper have their respective benefits, and we will likely need to use them in conjunction in future analysis efforts. With a deeper understanding of our simulations and usage of the analysis frameworks presented in this paper, we can uncover the best method of extracting the scattering length of liquid argon from the existing experimental data at wavelengths of 155 nm and lower.

At wavelengths higher than 155 nm, there is much work to be done to describe the behaviors exhibited. The behavior seen in Fig. 3 could be attributed to the cage's reflectivity, the time of day the data was taken, or some other unknown effect.

Provided an explanation of the high-wavelength discrepancies alongside the work presented in this paper, a promising measurement of the scattering length of liquid argon at varying wavelengths can be extracted from the LArS data with concentrated analysis work. This measurement would improve the simulation and reconstruction of scintillation light in large liquid argon experiments like DUNE.

VIII. ACKNOWLEDGMENTS

Dr. Alex Himmel was imperative to the work presented in this paper. He laid the computational and experimental foundations for the LArS experiment with assistance from other scientists and interns. Dr. Himmel also generated Fig. 2 and Fig. 3 of this paper.

c. This manuscript has been authored by Fermi Research Alliance, LLC under Contract No. DE-AC02-07CH11359 with the U.S. Department of Energy, Office of Science, Office of High Energy Physics.

d. This work was supported in part by the U.S. Department of Energy, Office of Science, Office of Workforce Development for Teachers and Scientists (WDTS) under the Science Undergraduate Laboratory Internships Program (SULI).

[1] A. I. Himmel, "Seeing Neutrinos: The Physics Potential of Photon Signals in DUNE," .

[2] L. Zhao, "Measurement of Rayleigh Scattering in Liquid Argon at Vacuum Ultraviolet Wavelengths," .

[3] S. Agostinelli *et al.*, "Geant4 - A Simulation Toolkit," Nucl. Instrum. Meth. A **506**, 250–303 (2003).

[4] J. A. et al., "Recent Developments in Geant4," Nucl. Instrum. Meth. A **835**, 186–225 (2016).

[5] J. A. et al., "Geant4 Developments and Applications," IEEE Trans. Nucl. Sci. **53**, 270–278 (2006).

[6] G. Seidel, R. Lanou, and W. Yao, "Rayleigh scattering in rare-gas liquids," Nuclear Instruments and Methods in Physics Research Section A **489**, 189–194 (2002).

[7] R. Brun and F. Rademakers, "ROOT - An Object Oriented Data Analysis Framework," Nucl. Inst. & Meth. in Phys. Res. A **389**, 81–86 (1997), proceedings AIHENP'96 Workshop, Lausanne, Sep. 1996. See also "ROOT" [software], Release v6.20.08a, 2020-03-04.

[8] A. Breaux, W. Mu, L. Zhao, W. Castiglioni, and F. Yu, "LArSMC," https://github.com/aihimmel/LArSMC (2025).